Accepted Manuscript

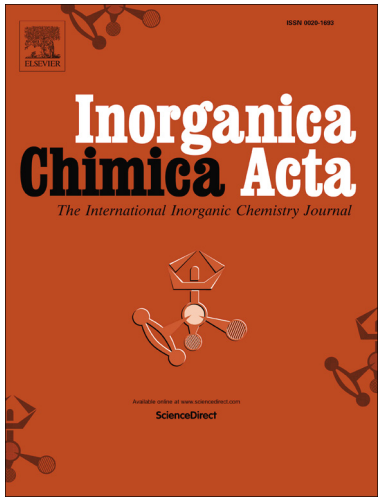

Research paper

Synthesis, Characterization, Cytotoxicity Effect and DNA Cleavage Study of Symmetric Dinuclear Chloro and Azido Bridged Copper(II) Complexes of Napthyl-pyrazole Based Ligand

Abhimanyu Jana, Paula Brandão, Gopinath Mondal, Pradip Bera, Ananyakumari Santra, Atish Dipankar Jana, Raveendra Babu Mokhamatam, Sunil Kumar Manna, Nandan Bhattacharyya, Pulakesh Bera

PII: S0020-1693(18)30468-7
DOI: https://doi.org/10.1016/j.ica.2018.06.054
Reference: ICA 18346

To appear in: *Inorganica Chimica Acta*

Received Date: 28 March 2018
Revised Date: 23 June 2018
Accepted Date: 29 June 2018

Please cite this article as: A. Jana, P. Brandão, G. Mondal, P. Bera, A. Santra, A.D. Jana, R.B. Mokhamatam, S.K. Manna, N. Bhattacharyya, P. Bera, Synthesis, Characterization, Cytotoxicity Effect and DNA Cleavage Study of Symmetric Dinuclear Chloro and Azido Bridged Copper(II) Complexes of Napthyl-pyrazole Based Ligand, *Inorganica Chimica Acta* (2018), doi: https://doi.org/10.1016/j.ica.2018.06.054

Synthesis, Characterization, Cytotoxicity Effect and DNA Cleavage Study of Symmetric Dinuclear Chloro and Azido Bridged Copper(II) Complexes of Napthyl-pyrazole Based Ligand

Abhimanyu Jana[a], Paula Brandão[b], Gopinath Mondal[a], Pradip Bera[a], Ananyakumari Santra[a], Atish Dipankar Jana [c], Raveendra Babu Mokhamatam[d], Sunil Kumar Manna[d], Nandan Bhattacharyya[e], Pulakesh Bera*[a]

[a]*Post Graduate Department of Chemistry, Panskura Banamali College, Vidyasagar University, Midnapore (E), West Bengal-721152, India*

[b]*Department of Chemistry, CICECO, University of Aveiro, 3810-193 Aveiro, Portugal*

[c]*Department of Physics, Behala College, Parnasree, Kolkata-700060, India*

[d]*Centre for DNA Fingerprinting & Diagonostics (CDFD),Hyderabad, Telengana–500 039, India*

[e]*Department of Biotechnology, Panskura Banamali College, Vidyasagar University, Midnapore (E), West Bengal-721152, India*

Abstract: Symmetric dinuclear chloro copper(II) complex $[Cu(L)(Cl)(\mu\text{-}Cl)]_2$ (**1**) and azo dinuclear azido copper(II) complex $[Cu_2(L)_2(N_3)_3(\mu_2\text{-}N_3)]_n$ (**2**) [where L represents (5-methyl-pyrazol-1-ylmethyl)-napthalen-1-ylmethyl-amine] have been synthesized to examine the effect of napthyl group in the structure of pyrazole based dinuclear copper(II) complexes in DNA nuclease activity. The structure of **1** and **2** are characterized by X-ray crystallography, electrochemistry and various spectroscopic techniques. Coordinating ligand L is generated in situ from bis(3,5-dimethyl-pyrazol-1-ylmethyl)-napthalen-1-ylmethyl-amine (A) during complexation. Cytotoxic potential of free ligand (A), synthesized complexes **1**, **2** and one cobalt(II) complex derived from ligand A, $Co^{II}(A)Cl_2$ (**3**) are analyzed using MTT cytotoxicity assay in U937 human monocytic cell line. Complexes **1** and **2** show very potent cytotoxicity (IC_{50} = 13–17 μM); the best IC_{50} value is found for **1**. LDH assay revealed that A and **3** has greater necrotic activity than the copper complexes. However, the results of DNA cleavage study clearly demonstrated that symmetric bridged dinuclear complexes with napthyl group lead to high level of nuclease activity 72–75% in the presence of glutathione. The bridged dinuclear copper(II) complexes undergo facile transformation to Cu(I) centre through inner sphere electron transfer mechanism (ISET) in presence of glutathione which facilitate the formation of free

radicals/ions for DNA cleavage. Lacking of any reducible metal center in mononuclear cobalt(II) complex make it inactive towards free radicals generation in DNA cleavage activity.

Key words: Bridged dinuclear; Copper(II) complexes; Napthyl pyrazole; DNA cleavage; Cytotoxicity

1. Introduction

Complexes with pyrazole based ligands are the subject of high valued research giving an opportunity for a better understanding on the structure-activity relationship in the active sites of metallo proteins. The metal ions in the biological systems are often coordinatively attached with one or more imidazole group which is the integral part of histidine unit of proteins. Pyrazole being isomeric with imidazole has the similar electronic and steric properties. Pyrazole/pyrazole derivatives can be prepared more easily than imidazole derivatives [1]. Therefore, much attention has been paid to the design of various pyrazole based coordination compounds ensuring special structural features to fulfil the specific stereochemical requirements for metal bonding [2]. Copper has been identified as a promising metal among the essential trace elements to interact with various pyrazole derived ligands for the biological studies [3–8]. Copper is involved in multiple functions of crucial enzymes and takes part as a fundamental unit of the redox system [9,10]. The advantage of using copper as the central atom for the preparation of potential metallo-therapeutics has already been established in a number of copper complexes, particularly those involving planar polydentate heterocyclic ligands. These complexes show notable cytotoxicity with varied model of DNA interaction mechanism and redox metabolism [11–15]. Many copper (II) complexes with N,N- and N,S- donor ligands have been reported as promising cytotoxic agents based on in vitro assay [16]. A series of copper(II)-thiolato mono and dinucleating ligands have been synthesized for biomimetic catalytic oxidation [17,18]. Pyrazole

and substituted bis(pyrazolyl) alkane ligands with N,N-donor sites are capable of showing high levels of cytotoxicity against HT 1080 (Human fibro sarcoma) cells [16]. The copper(II) complex with 3,5-dimethyl-1H-pyrazole-1-carbothiamide showed a tenfold higher cytotoxicity towards the melanoma A375 cell line than the reference *cis* platin. It was suggested that this complex could modify the structure of plasmid DNA by mimicking the DNA form [18]. DNA-proliferation studies induced by multinuclear copper(II) complexes were developed to model metalloenzymes [19] where a selective cleavage of the DNA backbone was executed by oxidation [20–23]. Isomeric pyrazole based derivatives are also studied for biological applications. J.A. Cowan showed oxidative cleavage of double-stranded DNA by imidazole based amino terminal copper(II) and nickel(II) complexes (ATCUN) [24]. A CuN_4 chromophore of copper(II) complexes with sulphonamide ligands degrades DNA in the presence of sodium ascorbate [25]. Dinuclear metal complexes with suitable bridging ligands show interesting catalytic promiscuity [26–28]. Dinuclear copper(II) complexes was evaluated using circular plasmid DNA and their cytotoxicity were assessed against selected human cancer cell lines. These complexes exhibited low DNA cleavage activity in the absence of additives inducing unique single-strand cleavage on plasmid DNA, together with moderate cytotoxicity against different tumour cell lines [29]. Methionine based Cu(II) complexes can promote a dual pathway for DNA. Probing the cytotoxic activity of these complexes on MCF-7, a human breast cancer cell line shows that one copper(II) complex is most effective with an IC_{50} of 70(2) nM [4]. In view of these facts, the precise nature of the ligand is of paramount importance in the interaction of the complex with the DNA molecule. The factors like metal-metal distance, redox potential, geometry around the metal centre, substitution with planar ring(s) and presence of labile sites essential for binding of substrate and/or availability of nucleophile need to be explored to

establish the probable mechanism associated with the native enzyme and proteins. Therefore, extensive studies with different structures are necessary in order to understand and evaluate the factors that determine the DNA cleavage mechanism. In this paper, we report on the synthesis of two new bridged copper(II) complexes derived from a tripodal napthyl-pyrazole ligand (NNN). The DNA interaction and binding study was done followed by structural, electrochemical and paramagnetic studies of complexes. Additionally, one mononuclear cobalt(II) complex (**3**) with the ancillary ligand A is also taken to compare the biological activities with the synthesized dinuclear complexes.

2. Experimental Section

*2.1*Reagents

The starting materials for the synthesis of the ligands like acetylacetone (Merck), hydrazine hydrate (Rankem), formalin (Merck), 1-methyl naphthylamine (Aldrich Chemicals) were of reagent grade and used as received. Copper (II) chloride dihydrate, copper (II) nitrate trihydrate (Merck, India) and sodium azide (Merck, India), were used for the preparation of complexes. Solvents like methanol, ethanol, chloroform, diethyl ether, acetonitrile (Merck, India) were of reagent grade and dried before use.

2.2 Synthesis

*2.2.1 Synthesis of bis-(3,5-dimethyl-pyrazol-1-ylmethyl)-naphthalen-1-ylmethyl-amine **(A)***

Compounds 3,5-dimethyl pyrazole and 3,5-dimethyl-1-hydroxymethyl pyrazole are required as precursors for the synthesis of ligand A, bis-(3,5-dimethyl-pyrazol-1-ylmethyl)-naphthalen-1-ylmethyl-amine. The preparation of 3,5-dimethyl pyrazole and 3,5-dimethyl-1-hydroxymethyl pyrazole are carried out by following the literature procedures [30]. The ligand A is synthesized by the condensation of 1-methyl naphthylamine (10 mmol, 1.57 g) and 3,5-dimethyl-1-hydroxymethyl pyrazole (20 mmol, 2.52 g) in 50 mL dry acetonitrile [31,32]. The water that is

produced during the condensation reaction is removed by drying over anhydrous Na_2SO_4. The supernatant liquid is separated out and filtered under reduced pressure, where a yellow oily mass is obtained. A white crystalline product is isolated after dissolution of the oily material in diethyl ether followed by cooling in the refrigerator. The white crystals were collected by filtration and dried in air. Yield is 75%. The purity of product is ascertained by ^{1}H NMR ($CDCl_3$, δ ppm): 1.63-2.28 (12H,s); 4.24 (2H,s); 4.93 (4H,s); 5.81 (2H,s); 7.28-7.83(7H,m).

2.2.2 Preparation of [Cu(L)(Cl)(μ-Cl)]$_2$ (**1**)

To a solution of A (1 mmol, 0.373 g) in 20 ml acetonitrile, solid $CuCl_2.2H_2O$ (1 mmol, 0.170 g) is mixed slowly with constant stirring for a time period of 30 minutes. The resultant green solid is filtered and dried in air. This solid residue is dissolved in mixed hot acetonitrile and methanol. This solution is kept in refrigerator for overnight where upon deep green crystals are separated out. The crystals are collected and dried over vacuum. Yield is 80%. CHN Analysis found (calcd.) for $C_{34}H_{38}N_6Cl_4Cu_2$: C, 51.20 (51.06); H, 4.55 (4.75); N,10.54 (10.51).

2.2.3 Preparation of [Cu$_2$(L)$_2$(N$_3$)$_3$(μ-N$_3$)]$_n$ (**2**)

Solid $Cu(NO_3)_2.3H_2O$ (1 mmol, 0.241 g) is allowed to mix with a magnetically stirring solution of A (1 mmol, 0.373 g) in 20 ml acetonitrile. To the resultant solution, 5 ml aqueous solution of NaN_3 (1 mmol, 0.065 g) is added drop wise. A dark brown solution was obtained and stirred for 3 hours at room temperature. Finally the solution is filtered and kept at room temperature allowing the slow evaporation. Dark brown single crystals suitable for X-ray crystallography are obtained. Yield is 55%. CHN Analysis found (calcd.) for $C_{34}H_{38}N_{18}Cu_2$: C, 49.10 (49.45); H, 4.50 (4.60); N, 30.25 (30.54).

2.2.4 Preparation of [Co(A)Cl_2](**3**)

The complex is prepared according to the process reported earlier [30]. In brief, an equimolecular mixture of A (10 mmol) and $CoCl_2 \cdot 6H_2O$ (10 mmol) is taken in methanol with constant stirring. The stirring is continuing for 3 h whereupon a solid is precipitated out. The product is filtered off and dried in vacuum. The solid is dissolved in hot methanol and acetonitrile mixture (1:1). The solution is filtered and kept in refrigerator to collect crystalline compound. Yield is 55%. This crystalline compound is taken for the experiment.

2.3 **Physical Measurements**

Elemental analysis (C, H, N) were carried out using FISONS EA-1108 CHN analyzer. UV-Vis spectra of the complex were measured using a Perkin Elmer Lamda-35 spectrophotometer with a 1 cm path length quartz-cell. Thermogravimetry analysis of **1** and **2** were performed using Perkin Elmer analyser Model TGA 4000 using nitrogen gas at a heating rate 10 °C/min.

2.4 **X-ray crystallography**

Single crystal X-ray data of **1** and **2** were collected at 150 K temperature on a Bruker SMART APEX-II CCD diffractometer using graphite monochromated MoK_α radiation (λ= 0.71073Å). The crystals were positioned at 40 mm from the CCD and the spots were measured using 5 s and 25 s counting time, respectively. Complex **2** is twin and it was indexed using Cell Now program [33, 34]. Data integration and reductions were processed with SAINT$^+$software [35]. Multi-scan absorption correction was applied to all intensity data using the SADABS program for complex **1** and TWINABS program for complex **2** [36]. Structures were solved by the direct method and then refined on F^2 by the full matrix least square technique with SHELX-2013software [37]. All the non-hydrogen atoms were refined using anisotropic thermal parameters. The C-H hydrogen atoms were included at calculated positions and refined with isotropic parameters equivalent to 1.2 times those of the atom to which they are attached. The hydrogen atoms bonded to the

nitrogen atoms for both complexes (N3, N3a and N3b) were obtained from the last final difference Fourier maps.

2.5 **Electrochemistry**

Electrochemical studies were carried out with a CH electrochemical work station model CHI630E, using methanol in presence of tetra butyl ammonium perchlorate as a supporting electrolyte. The conventional three electrode assembly is comprised of a glassy-carbon working electrode, a platinum wire auxiliary electrode and a Ag/AgCl reference electrode. The electrochemical data of complexes (10^{-3} M) were recorded using 0.1 M TBAP at a scan rate 100mV/s.

2.6 **DFT study**

For understanding the electronic structure of the napthyl-pyrazole ligand and both the complexes **1** and **2**, geometry optimization was carried out for each one. All calculations were performed using the GAUSSIAN package [38]. Initial geometries of the ligand and the complexes were adopted from the crystal structure and geometry optimization for each one has been carried out at the DFT 6-311G level of theory with B3LYP hybrid density functional.

2.7 **EPR study**

The X-band electron paramagnetic resonance (EPR) spectrum was recorded in a Bruker EMX X-band spectrometer operating at a field modulation of 100 kHz, modulation amplitude of 7 G and microwave radiation power of 10 mW at 90K.

2.8 **Biological Assay**

2.8.1 Cytotoxicity assay

The cell cytotoxicity of the complexes was assessed using MTT, 3-(4,5-dimethylthiazol-2-yl)-2,5-diphenyltetrazolium bromide, assay based on the ability of mitochondrial dehydrogenage in the viable cells to leach the tetrazolium rings of MTT and forming dark blue membrane-

impermeable crystals of formazan that could be measured spectrophometrically. The formazan product formed gave a measure of the number of viable cells. About 5000 cells/well of human histiocytic lymphoma U937 were plated in a 96 well plate and treated with different concentrations of ligand (L) and copper compounds **1**, **2**. After 72 h of incubation of the sample in a CO_2 incubator, 20 µL of MTT dye (5 mg/mL in PBS) was added per well, and incubation was continued for 3 h at 37 °C. The culture medium was discarded, and 100 µL of lysis buffer (20% SDS in 50% dimethylformamide) was added and kept for 1 h on a shaking rocker to solubilize the cell membrane and dissolve the formazan crystals. The absorbance at 595 nm was determined using a microplate reader. The cytotoxicity of the test compounds were measured as percentage ratio of the absorbance of the treated cells over the untreated controls. The IC_{50} values were determined by nonlinear regression analysis using Graphpad Prism software.

2.8.2 **Lactate dehydrogenase (LDH) release assay**

LDH is a cytosolic enzyme which is released into culture supernatant upon induction of necrosis of cell. U937 cells were treated as stated earlier in the cytotoxicity assay experiment [39]. The culture supernatants were isolated and LDH activity was assayed after 20 minutes incubation at 25°C with substrate solution (30 mM sodium pyruvate and 6.6 mM NADH in 0.2 M Tris-Cl buffer, pH 7.3). The absorbance of the solutions were measured at 340 nm. The LDH activity was indicated as relative cytolysis of the compound treated cells from a plot considering absorbance of triton X-100 treated cells as 100%.

2.8.3 **DNA cleavage experiments**

Cleavage of supercoiled pEGFP-C3 (4.7 kb) DNA (0.4 µg, 4727 base pairs) was studied by agarose gel electrophoresis using copper complexes in 50 mM tris(hydroxymethyl)-methane-HCl (Tris-HCl) buffer (pH 7.2) containing 50 mM NaCl. The chemical nuclease activity of the

complexes was studied using hydrogen peroxide (200 μM) as an oxidizing agent and glutathione (GSH, 1 mM) as the reducing agent. Each sample was incubated for 1.0 h at 37 °C and analyzed for the cleaved products using gel electrophoresis following procedures reported earlier [24]. The extent of DNA cleavage was calculated from the intensities of the bands using the UVITEC Gel Documentation System. Due corrections were made for the low level of nicked circular form present in the original supercoiled DNA sample and for the low affinity of EtBr binding to supercoiled compared to nicked circular and linear forms of DNA. The concentrations of L, **1** and **2** (10 μL) corresponded to that in the 20 μL final volume of the sample using tris buffer. The mechanistic studies were carried out by adding various additives (DMSO, 0.4 M; glycerol, 0.4 M; histidine, 0.1 M; sodium azide, 0.1 M; catalase, 10 μg/ml) prior to the addition of the ligand/complex.

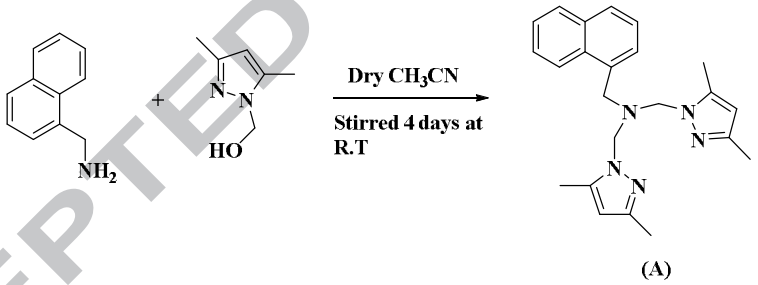

(A)

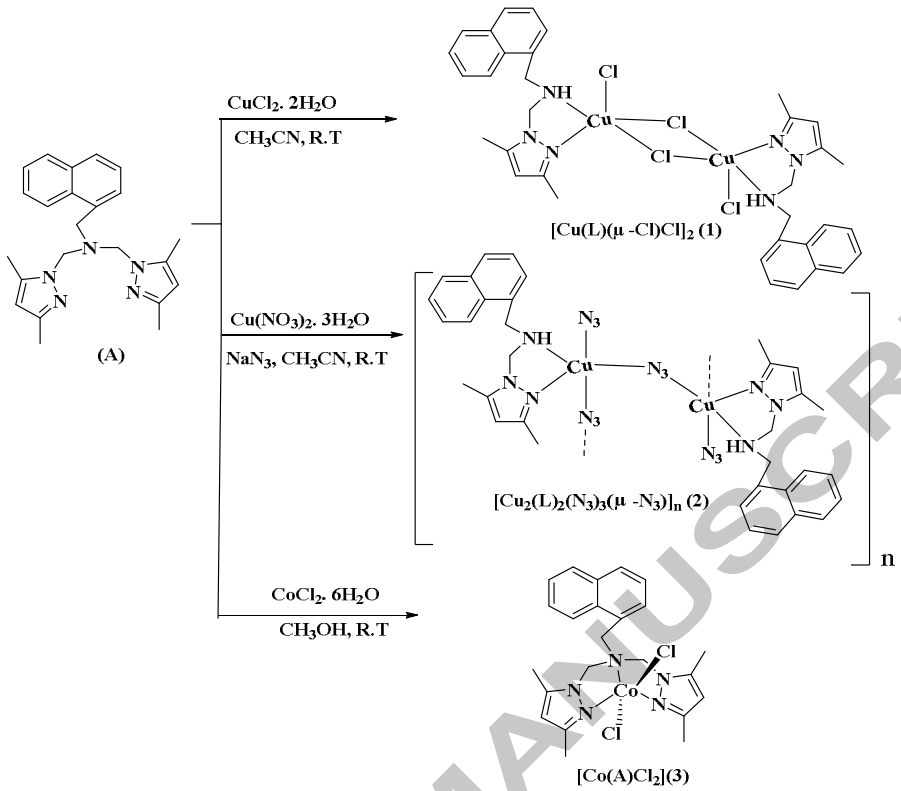

Scheme 1: Reaction scheme of ligand and complexes **1, 2** and **3.**

3. Results and discussion

3.1 Syntheses and general characterization

The tripodal napthyl-pyrazole based ligand (A) was synthesized by the condensation of (3,5-dimethyl-1H-pyrazol-1-yl)methanol with 1–methyl naphthylamine in a 2:1 molar ratio in acetonitrile. The elemental analysis, mass and NMR spectroscopy and structural characterization of its cobalt(II) complex were reported earlier [32]. In the reported cobalt(II) complex the ligand A binds as NNN tridentate neutral donor without showing any kind of dissociation upon complexation. But the reaction of ligand A with $CuCl_2.2H_2O$ or $Cu(NO_3)_2.3H_2O/NaN_3$ furnishes crystalline dinuclear copper(II) complexes where the parent ligand A undergoes dissociation to L under the reaction conditions. It may assume that the methanol in presence of chloride and azide ions facilitates the removal of a pyrazole moiety. Similar kind of transformations of the parent

ligand were also observed [40–43]. One pendant arm of the tridentate ligand (A) was removed by cleaving C–N (amine) bond towards the formation of a stable system of a dinuclear complex of L. This dissociation of ligand prior to formation of metal complexes is evidenced by the presence of an m/z value of 127 (MH^+ peak) corresponding to 3,5–dimethyl pyrazole 1–carbinol in the GC-Mass spectrum (Fig S1). The reasons are by no means certain but no doubt several factors are involved, of which size of the ligand is probably a major one. Being a smaller donor (N-donor) than A (Scheme 1), L prefers to stabilize the bridged $Cu^{II}L$ complex rather than a mononuclear $Cu^{II}A$ complex. There is a delicate balance between formation of chelate with undissociated ligand (A) and formation of polynuclear chain with dissociated fragment L. High polymerization effect that includes the hydrogen bonding in the system outweighs the combined effects of chelate formation and ligand dissociation leading to the formation of a relatively stable polynuclear chain structure. The strong intermolecular interactions also give the thermodynamic stability of the chloro/azido bridged complexes. An optimization of dissociated L was performed to check the possibility of the formation of L in the system. The optimized geometry, HOMO and LUMO of the ligand has been depicted in Fig. 1. The computer generated geometry of L is close to that of the ligand coordinated to the copper centre in the crystal structures of **1** and **2**. Its HOMO is spread over the whole molecule but LUMO is mainly concentrated over the napthyl moiety of the ligand. The bond lengths corresponding to the optimized geometry of L in the complexes are summarized in the supplementary material (Table S1 and S2).

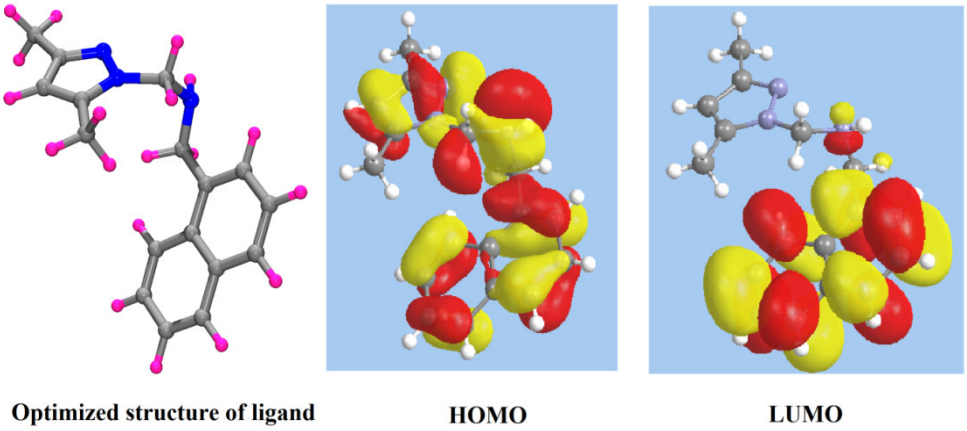

Fig. 1 The optimized structure of L showing HOMO and LUMO

3.2 Thermogravimetry analysis

The thermal decomposition of the complexes is performed in nitrogen atmosphere with sample of amount 1 mg at a heating rate 10 °C/min. As shown in Fig. **2**, the TG curve of **1** has two major decomposition steps. The first step of decomposition in the temperature range 170– 240 °C is 35.22% of total mass which corresponds to the loss of two methylene naphthalene units (*ca.* 35.26%). In the second step, a combined mass loss occurs due to losses of two unit of amino methyl pyrazole (*ca.* 31.01%) and $2Cl_2$ (*ca.* 17.75%) giving a residue of two unit of metallic copper (*ca.* 15.88%). A plausible mechanism of decomposition is shown in Scheme 2. As shown in Fig.2, complex **2** approximately shows three steps of decomposition. The first step of decomposition refers to the loss of four moles of coordinated azide (*ca.* 20.34%) followed by the loss of two methyl naphthalene units (*ca.* 34.14%). The last step of the decomposition confers the loss of organics i.e., amino methyl pyrazole unit (*ca.* 30.02%) giving residue of two units of metallic copper (*ca.* 15.37%). It is reasonable to assume that the breaking of weakly bridging bonds is taking place before any kind of major loss in the reported complexes (Scheme 2).

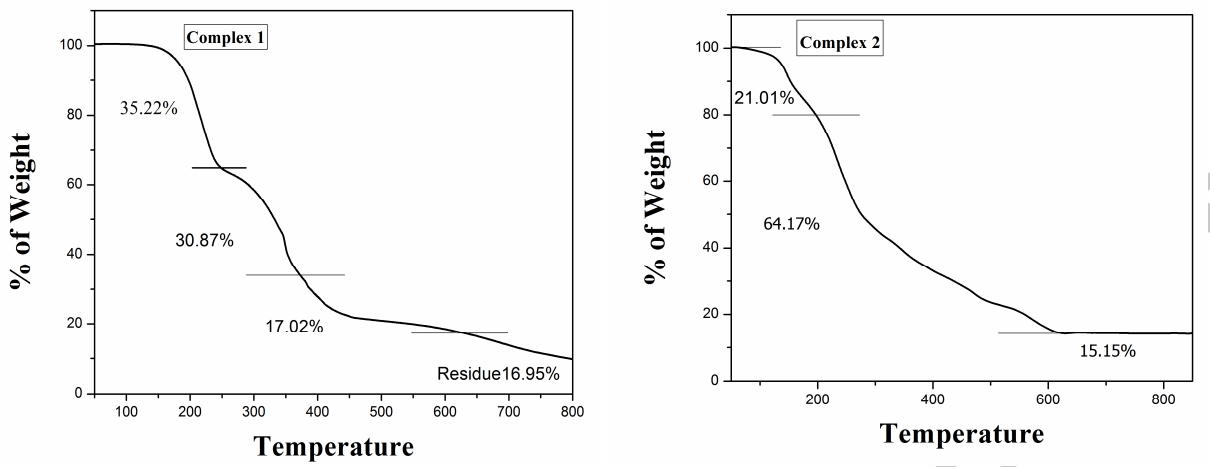

Fig.2: TG of complex **1** and **2** in nitrogen atmosphere with sample of amount 1 mg at a heating rate 10°C/min

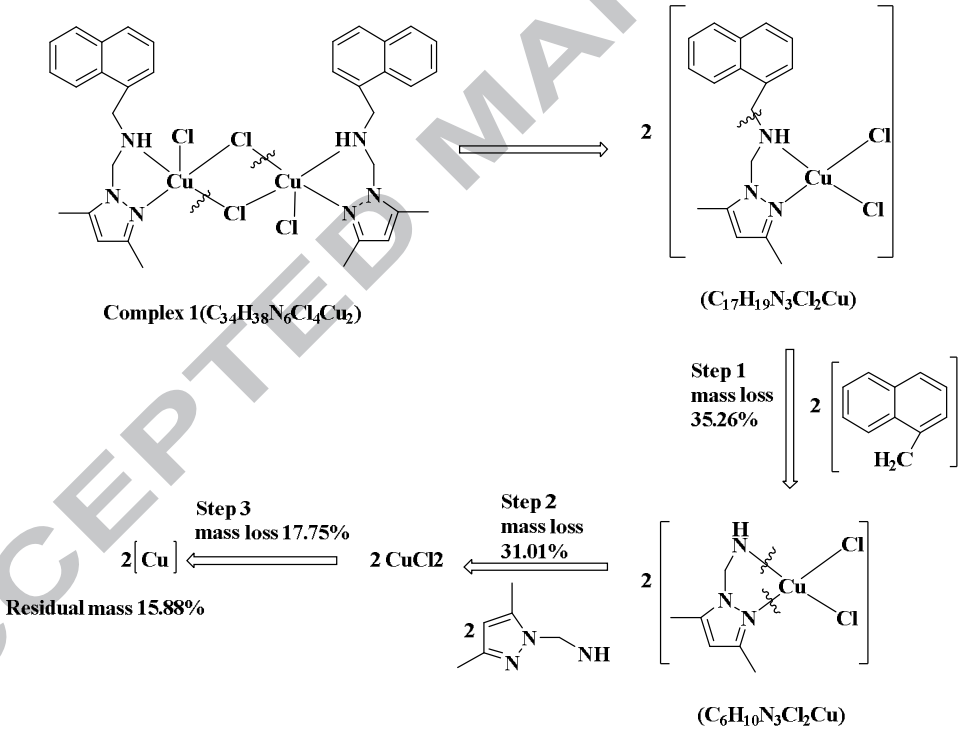

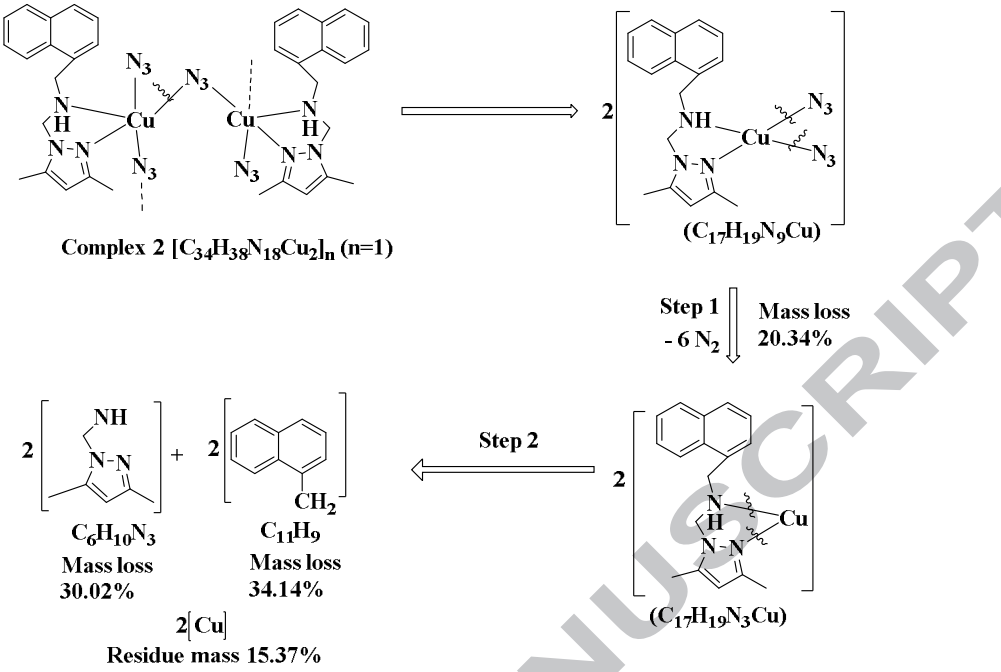

Scheme 2: Plausible mechanism of decomposition of **1** and **2**

3.3 **Electrochemistry**

Cyclic voltammetry (CV) experiments of complexes **1** and **2** in methanol solution with a scan rate of 100 mV s^{-1} showed multiple reduction and oxidation peaks as shown in Fig. 3. As shown in Fig. 3a, complex **1** displayed reductive responses at C1(0.38V) and C2(0.75V) which can be attributed to Cu(II)/Cu(I) and Cu(I)/Cu(0) complexes, respectively. The corresponding reversible oxidative response were observed at A1(0.55V) and A2(0.93V) for the redox couple Cu(II)/Cu(I) and Cu(I)/Cu(0), respectively, during the anodic potential scan as shown in Scheme 3. Similar oxidative and reductive responses were also obtained for complex **2** (Fig. 3b) [44, 45]. The details of peak potential values and $E_{1/2}$ values for both complexes are listed in Table 1. Therefore, it may be assumed that the Cu(II) centres of the complexes are first reduced to Cu(I) and in the last step the Cu(I) is finally reduced to Cu(0). It is to be noted that complex **3** shows one irreversible peak at 1.52V corresponding to the Co(III)/Co(II) redox couple (Fig. S2). The results indicate that complexes **1** and **2** are more susceptible to reduction than complex **3**.

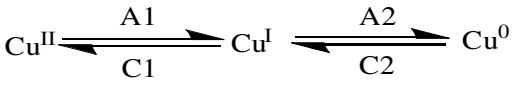

Scheme 3: Redox couple Cu(II)/Cu(I) and Cu(I)/Cu(0).

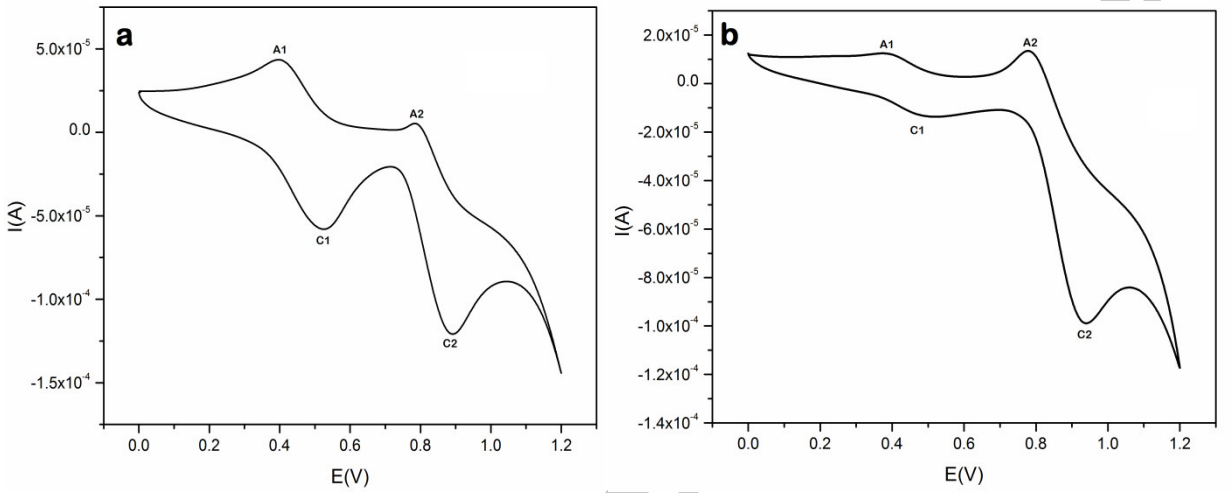

Fig. 3 Cyclic voltammogram of **1** (a) and **2** (b) in methanol and TBAP (0.1 M) as a supporting electrolyte at a scan rate 100mV/s.

Table 1 **Cyclic voltammogram data for** 1 **and** 2 in methanol and TBAP (0.1 M) as a supporting electrolyte at a scan rate 100mV/s.

Complex	E_{pA1}	E_{pC1}	$(E_{1/2})^1$	E_{pA2}	E_{pC2}	$(E_{1/2})^2$
1	0.38V	0.55V	0.46V	0.75V	0.93V	0.84V
2	0.38V	0.49V	0.43V	0.77V	0.93V	0.85V

3.4. EPR spectroscopy

The EPR spectroscopy of copper(II) complexes is a useful tool to study the electronic environment of the complex and the mechanistic pathway involved in a reaction. Generally, copper(II) complexes have a distorted octahedral geometry (tetragonal or rhombic) giving an

axially symmetric more intense peak at higher field ($g_\perp$) and a less intense peak at lower field ($g_\parallel$). The X-band EPR spectra of **1** and **2** show a characteristic four line signals for a coupled dinuclear complex (Fig. 4). The X-band EPR spectrum of **1** in DMF at 90 K shows a slightly rhombic distorted spectrum with $g_\perp$ and $g_\parallel$ values of 2.10 and 2.30, respectively with a hyperfine splitting ($A_\parallel$) value of 150G (Fig. 4a). Thermally accessible higher energy triplet states ($2J \approx KT$) (where 2J refers to the energy differences between triplet states) is give rise to transitions at 2750, 2921 and 3071 G indicating antiferromagnetic coupling of the two Cu(II) centres [46,47]. A similar feature is also observed in the EPR spectrum of **2** in DMF (Fig.4c). In the solid state spectrum of **1,** an anisotropic peak is observed with $g_\perp$ and $g_\parallel$ values of 2.10 and 2.30, respectively at 90 K where only one broad peak observed in the lower G value instead of hyperfine couplings or a zero-field splitting interaction (Fig. 4b). However, the anisotropic hyperfine features (three lines) are observed in the solid state spectrum of **2** with $g_\perp$ and $g_\parallel$ values of 2.09 and 2.47, respectively at 90 K. This fact can be explained because the Cu…Cu distance of **2** is about 0.19 Å greater than in **1** which reveals that **2** is magnetically more diluted than **1**. Generally, the solid state samples are magnetically non-diluted and hyperfine couplings or zero-field splitting are absent (29). In both complexes, the $g_\parallel > g_\perp$ values suggest a square pyramidal copper(II) environment with the unpaired electron located in the $d_{x^2-y^2}$ orbital.

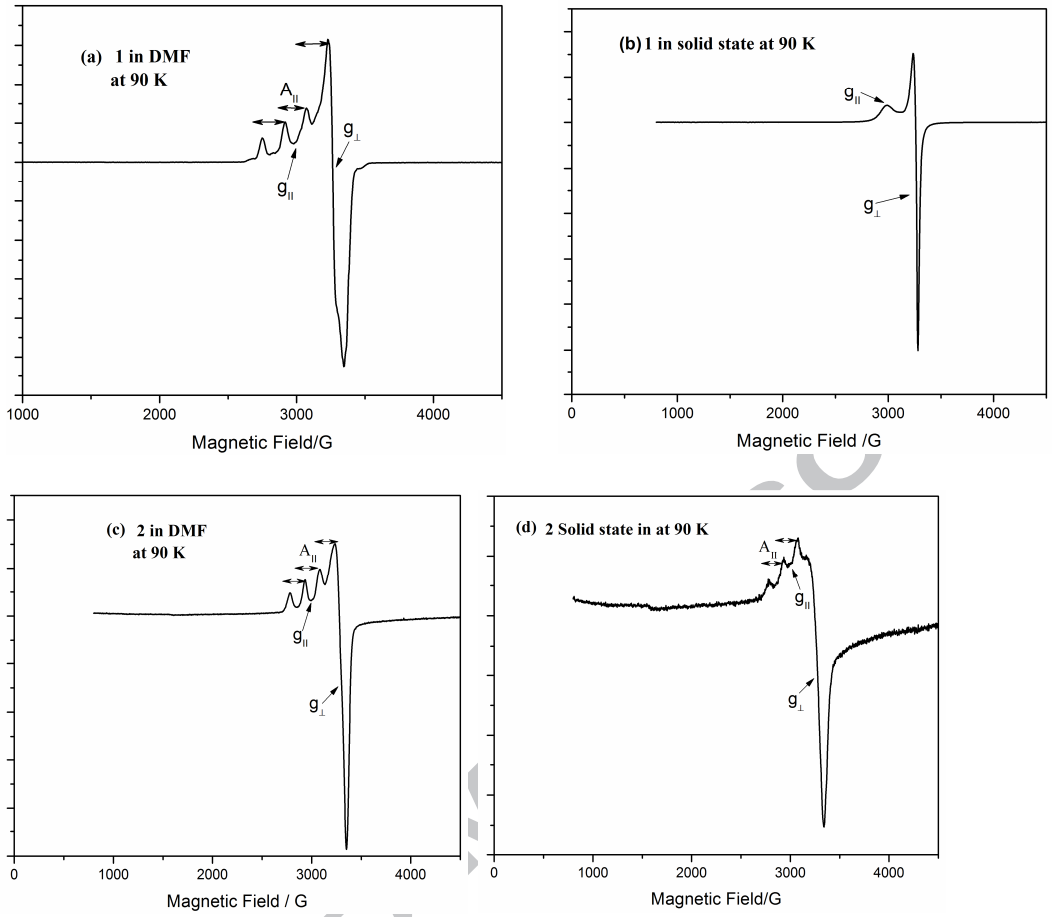

Fig. 4: The X-band EPR spectra in DMF (a), in solid state (b) of **1**; **t**he X-band EPR spectra in DMF (c) and in solid state (d) of **2** at 90 K.

*3.5 Structural description of **1** and **2***

The ORTEP diagram of complex **1** with atom numbering scheme is shown in Fig. 5 and crystal refinement parameters are shown in Table 2. Single crystal X-ray structure of complex **1** reveals a chloro bridged centrosymmetric dinuclear Cu(II) unit as the basic molecular complex. The coordination environment of each Cu(II) ion is nearly square pyramidal. In each of the five coordinated Cu(II) units, the square base plane is formed by two N atoms of L and two bridging Cl^- ions. The remaining axial position of square pyramid is occupied by another Cl^- ion. Selected bond lengths as well as bond angles are listed in Table S2. The basal plane bond distances Cu-

N1, Cu-N3, Cu-Cl1(μ_2) and Cu-Cl_2 are 2.003(Å), 2.060(Å), 2.285(Å) and 2.719 (Å), respectively. The basal angles N1-Cu-N3 = 80.72(6)° , N3-Cu-Cl1=89.67(4)°, Cl1-Cu-Cl2=93.68(2)°, Cl2-Cu-N1=97.47(4)° and the apex to basal angles Cl1*-Cu-N1=104.74(4)° (*=1-x, 1-y, 1-z), Cl1*-Cu-N3=83.10(4)°, Cl1*-Cu-Cl1=95.28(2)°, Cl1*-Cu-Cl2 =95.96(2)°. The nature of distortion of the coordination environment from perfect square pyramidal around the copper(II) centre is evident in the ligand-metal-ligand bite angles that vary around 90° with a range spread not exceeding 10°. Cu(II) ion is situated 0.155(1) Å below the mean plane passing through N1, N3, Cl1 and Cl2. The extent of distortion of the coordination polyhedron from the square pyramid to the trigonal bipyramid is generally given by the index τ defined as $\tau = \beta - \alpha/60$ where β and α are the two trans basal angles [47]. In the present case the τ value equals to 0.31, corresponding a copper(II) square pyramidal coordination polyhedron. The napthyl ring as well as pyrazolyl rings are disposed trans to each other with respect to the rigid $Cu_2(\mu_2\text{-}Cl)_2$ unit giving a centre of symmetry to the molecule. The trans disposed napthyl or pyrazole rings might be helpful for effective interaction with DNA molecules.

Dinuclear units self-assemble through two sets of cooperative CH···π interactions and are organized into a 2D supramolecular assembly in the (101) plane. Both the pyrazolyl methyl groups are involved in CH···π interactions. One of these interacts with the napthyl inner ring, leading to the 2D assembly which is reinforced by CH···π interaction of the ligand -CH_2 part with the outer napthyl ring (Fig. S3). Geometrical parameters corresponding to these interactions have been summarized in Table S3. The CH···π interaction mediated by the opposite methyl group attached to the pyrazole moiety lead to stacking of the (101) layers in the [101] direction (Fig S4). The separation between the planes is 10.178 Å. The stacking assembly is the result of

cooperation of the above mentioned CH···π interaction and the CH···Cl hydrogen bond (Table S3, Table S4).

The X-ray crystal structure of complex **2** shows the presence of a dinuclear $[Cu_2(L)_2(\mu_{1,1}\text{-}N_3)(\mu_{1,3}\text{-}N_3)_2]$ unit (Fig.6) as the asymmetric unit which is a part of a 1D coordination polymeric chain (Fig. S5). The neutral ligand L acts as a bidentate chelating agent for each of the copper centers [Cua and Cub] which are bridged by two a set of azide ions. Furthermore, Cua and Cub bridge with a neighbouring Cu centre through $\mu_{1,3}$ N7-N8-N9 and N13-N14-N15 azide ions, respectively. The two types of bridges e.g., end-on and end-to-end are extended into a 1D coordination polymer. The coordination environment for each copper centre is best described as a distorted square pyramid. The basal plane of the square pyramid around Cua is formed by two N atoms [N1A and N3A] of ligand L, one N atom [N4] of the $\mu_{1,1}\text{-}N_3$ group and another nitrogen atom (N7) of the $\mu_{1,3}\text{-}N_3$ groups. The axial position of the square pyramid around Cua is satisfied by the N13 atom of the azide in an end to end bridging fashion. Similarly, the basal plane of the square pyramid around Cub is formed by two N atoms [N1B and N3B] contributed by the chelating ligand L, and two N atoms [N10 and N13] contributed by the pair of azide ions. The axial position of the square pyramid around Cub is occupied by N4 of the $\mu_{1,1}$-azide ion. The Cu-N (ligand) distances vary in the range of 1.94–2.10 Å, which falls in the usual Cu–N bond range in the reported papers (Table S2). On the other hand, Cu-N (azide) distances in the basal plane vary from 1.95–2.34 Å, which also fall in the usual range. The axial Cu–N (azide) bond distances are 1.94 Å and 2.35 Å, respectively. Typical bond angles characterizing the square pyramidal coordination environments of Cua and Cub have been summarized in Table S2 which shows a slight deviation of the coordination square pyramid from its ideal geometry. The Cua atom is drawn towards the apex from the mean basal plane passing through N1A, N3A, N7 and

N4 atoms by 0.136(1)Å. Similarly, Cub is away from the mean basal plane passing through N1B, N3B, N10, N13 atom by 0.126(1) Å in the direction of the apex of the coordination polyhedra around Cub. The τ value of the distorted square pyramid around Cua is 0.06 and that of Cub is 0.03. It is to be noted that τ = 0 for a perfect square pyramidal geometry [47]. Here, the Cui...Cuj separation along the 1D coordination polymeric chain is 3.577Å and 5.644Å through end-on bridging and end-to-end bridging azides, respectively. It is interesting to note that the end-on bridging by two azide ions is not identical. In the Cua-N4-Cub bridge, the stronger bridging is reflected by the shorter bond distances (Cua-N4=1.953Å, Cub-N4=2.32 Å and angle Cua-N4-Cub=113.08(14)°) compared with the Cua-N13-Cub bridge (Cua-N13=3.064Å, Cub-N13=2.002Å and angle Cua-N13-Cub = 87.19°). Coordination polymeric chains run along the crystallographic *a*-axis. The chain is propagated due to successive end-on and end-to-end azido bridging. The end-to-end azido bridging is reinforced by N-H···N hydrogen bonding (Fig S5, Table S4). Successive polymeric chains are joined at the edges due cooperative CH···π and π···π interaction (Fig S5, Table S3, Table S5) leading to a supramolecular assembly along the (011) plane. These (011) planes are further assembled by another set of CH···π interaction leading to the final stacking of these planes along the [011] direction (Fig. S6).

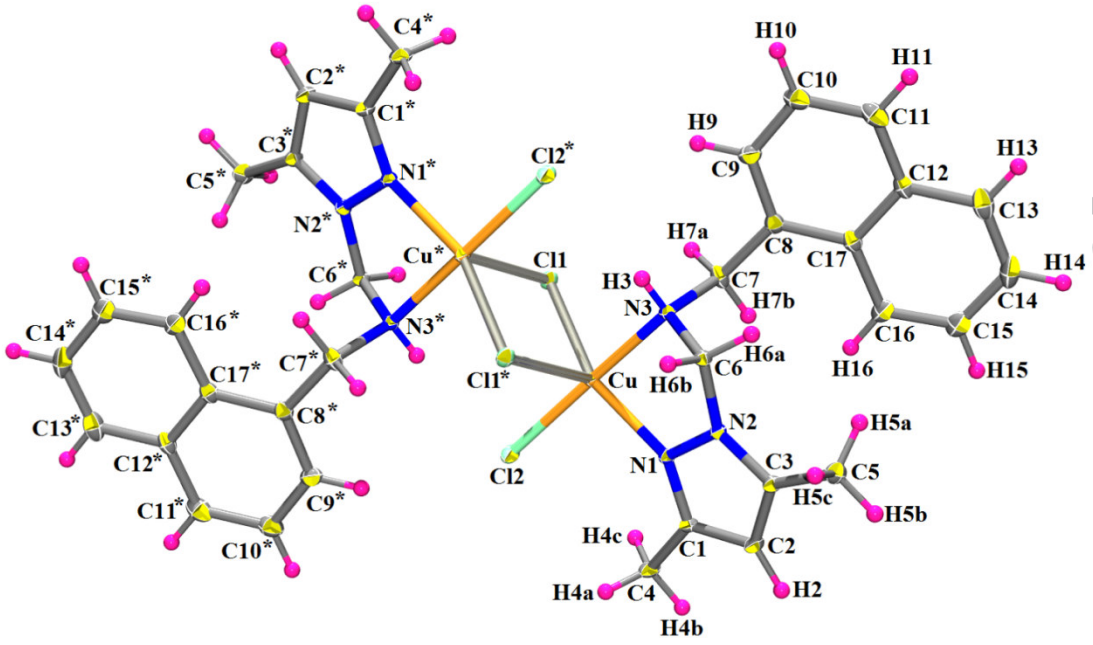

Fig. 5 ORTEP diagram of **1** (30% ellipsoidal probability) with atom numbering scheme. (Symmetry code * = 1-x, 1-y, 1-z)

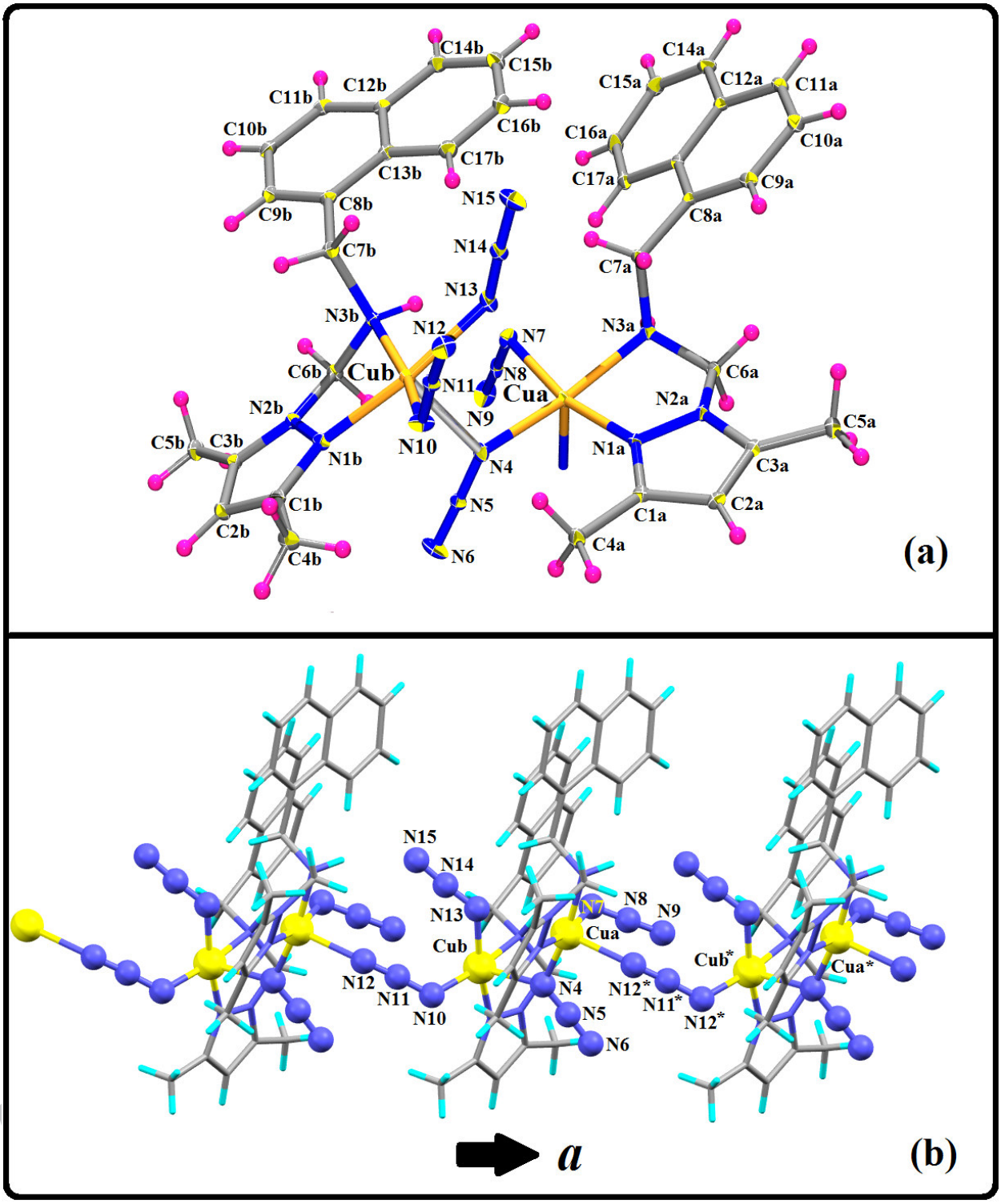

Fig. 6 (a) ORTEP diagram (30% ellipsoidal probability) of an excerpt Of **2** with atom numbering scheme. (b) Azido bridged polymeric chain running along the crystallographic *a*-axis. (symmetry code * =1+x, y,z)

Table 2 Crystal data and Refinement parameters of **1** and **2**

Crystal Data		
	1	**2**
CCDC	1551718	1551717
Formula	C_{34} H_{38} Cl_4 Cu_2 N_6	C_{34} H_{38} Cu_2 N_{18}
Formula Weight	799.60	825.92
Crystal System	monoclinic	Triclinic
Space group	$P2_1/n$ (No. 14)	P1 (No. 1)
a, b, c [Å]	11.8067(7) 9.0081(5) 16.1868(9)	8.2229(7) 10.5534(10) 11.6684(11)
alpha, beta, gamma [◦]	90 100.274(2) 90	63.751(3) 89.079(3) 77.329(3)
V [$Å^3$]	1693.96(17)	882.25(14)
Z	2	1
D(calc) [g/cm^3]	1.568	1.554
Mu(MoK_α) [/mm]	1.606	1.261
F(000)	820	426
Crystal Size [mm]	0.06 x 0.28 x 0.30	0.03 x 0.16 x 0.16
Data Collection		
Theta Min-Max [◦]	2.3, 29.2	2.2, 28.1
Dataset	-14: 16 ; -12: 12 ; -22: 22	-10: 10 ; -12: 13 ; 0: 15
Tot., Uniq. Data, R(int)	23100, 4594, 0.027	4264, 4264, 0.046
Observed data [I > 2.0 σ(I)]	4183	4182
Refinement		
Nref, Npar	4594, 214	4264, 500
R, wR2, S	0.0315, 0.0847, 1.07	0.0229, 0.0614, 1.06
	$w = 1/[\sigma^2(F_O^2)+(0.0428P)^2+1.6653P]$ where $P=(F_O^2+2F_C^2)/3$	$w = 1/[\sigma^2(F_O^2)+(0.0358P)^2+0.2518P]$ where $P=(F_O^2+2F_C^2)/3$
Max. and Av. Shift/Error	0.00, 0.00	0.00, 0.00
Min. and Max. Resd. Dens. [e/ $Å^3$]	-0.40, 1.29	-0.37, 0.38
Flack x	-	0.094(6)

The optimization of the structure of dinuclear copper complexes is done to compare the structural parameters to that of the results from X-ray crystallography. The optimized structure of **1** and corresponding HOMO and LUMO are depicted in Fig.7. The computed bond lengths and angles for the complex are systematically larger (Table S1) but the overall optimized geometry of the complex is same as that in the crystal structure. Both HOMO and LUMO of **1** are concentrated around the bridged dinuclear Cu units. Contribution to HOMO and LUMO is mainly due to Cu ions and chloride ions. In case of complex **2**, the repeating azido bridged dinuclear Cu(II) units of the coordination polymeric chain were isolated from the crystal structure and were taken as initial input for the optimization. The optimized structure of this

azido bridged dinuclear unit of **2**, corresponding HOMO and LUMO are depicted in Fig. 8. The computed bond lengths and angles for the complex are systematically larger (Table S2) again. The overall optimized geometry of the complex correlates nicely with that found in the crystal structure. Like complex **1**, here also both HOMO and LUMO are concentrated around the bridged dinuclear Cu units. Contribution to HOMO and LUMO is mainly by Cu ions and azide ions.

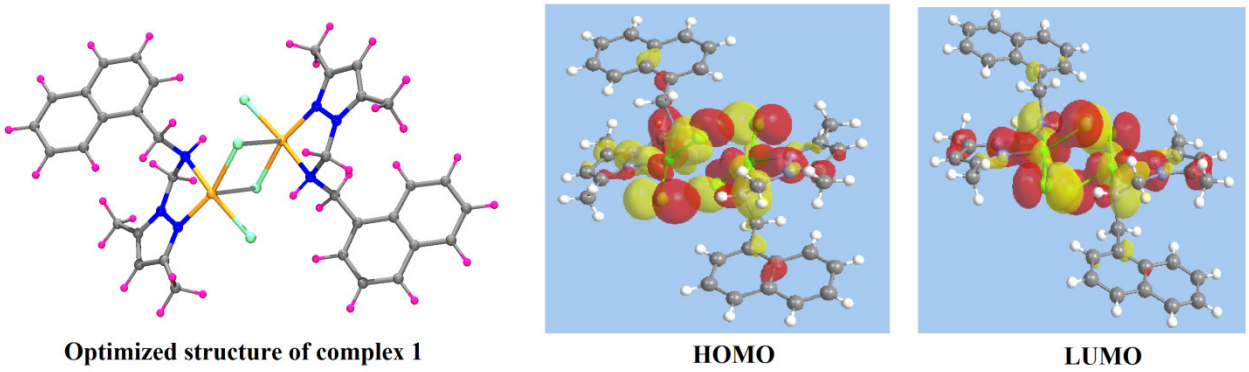

Fig. 7 The optimized structure of **1** and corresponding HOMO and LUMO

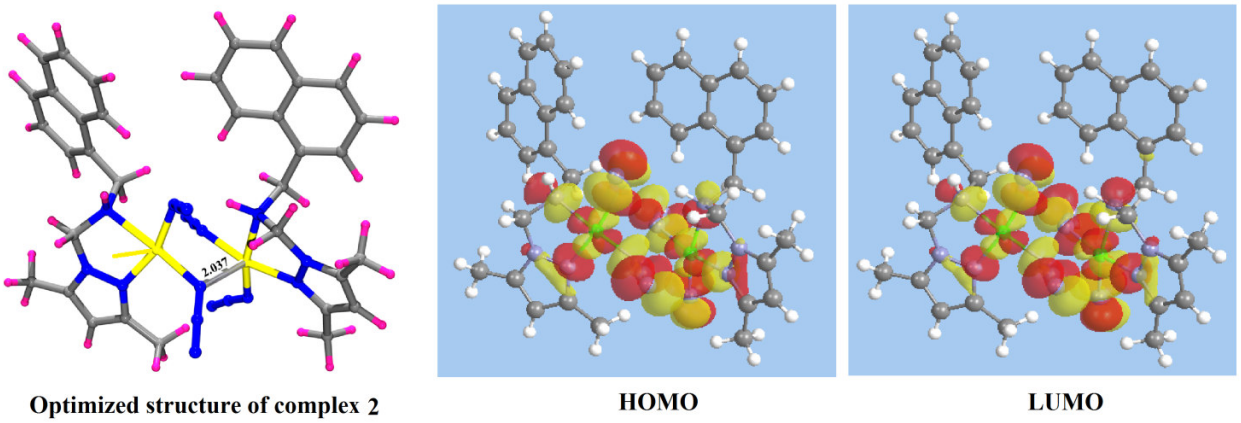

Fig. 8 The optimized structure of dinuclear excerpt of **2** and corresponding HOMO and LUMO

3.6 **Cytotoxicity assay**

U937 human monocytic cells were treated with the ligand L and the complexes **1** and **2** to probe the ex vivo cytotoxicity using MTT cytotoxicity assay. At the same time the cytotoxicity assay was performed with the reported mononuclear cobalt(II) complex, $[Co(A)Cl_2]$ (**3**) to compare the

effect with the copper(II) complexes. The ligand A is an effective cytotoxic agent against U937 human monocytic cell line with an IC50 of 23±2 µM (Fig.9A); but its derivatives are more potent than the ligand as they are showing smaller IC_{50} values. However, the copper derivatives of L are quite potent in inhibiting cell proliferation showing IC50 values ranging from 13±1 to 18±4 µM. Complex **1** is the most potent compound among the copper complexes with an IC_{50} value 13±1 µM (Fig. 9C) whereas complexes 2 and 3 show potentiality with IC_{50} values of 17±3 µM and 18±4 µM, respectively (Fig. 9B and 9D).

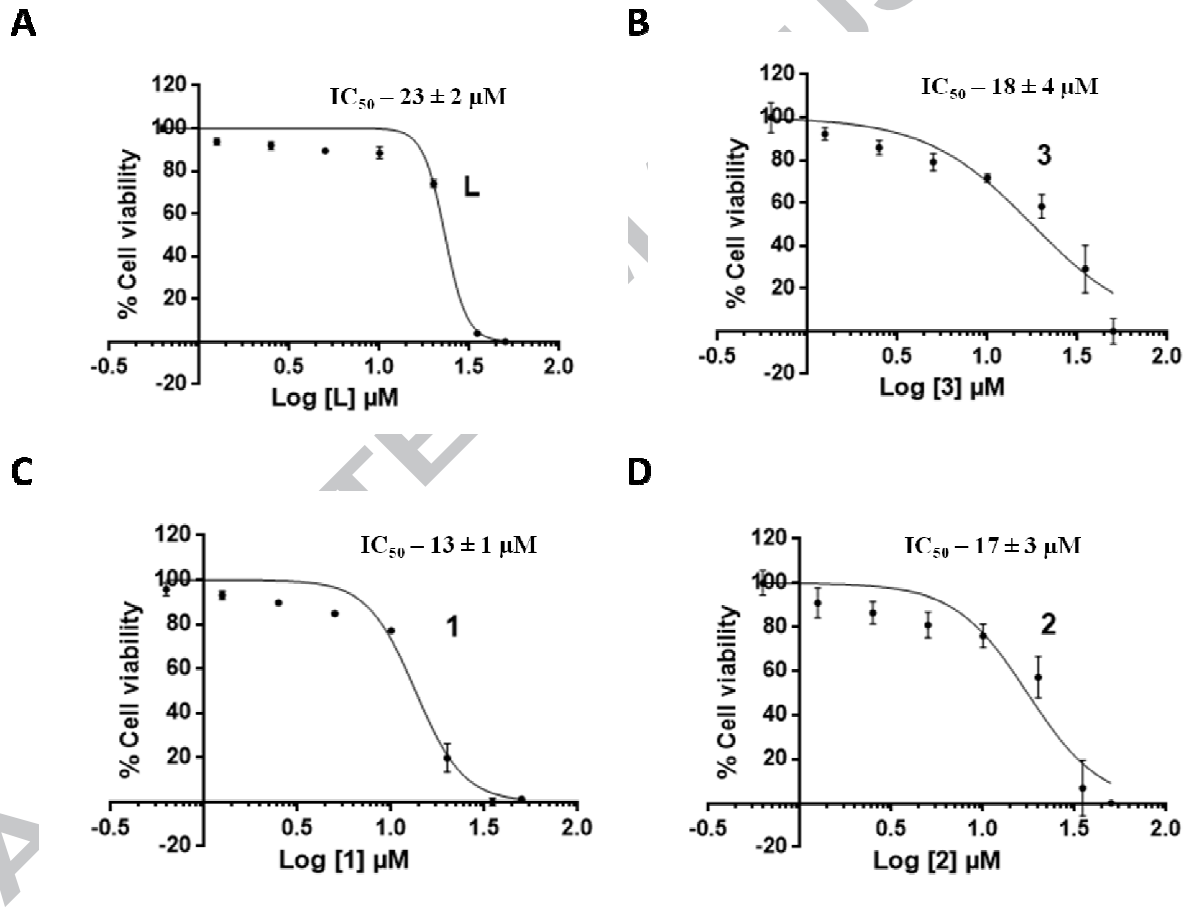

Fig. 9 Effect of compounds on cytotoxicity of U937 cells. U937 cells were treated as shown above for 72 h, with different concentrations of (A) Ligand A, (B) **3**, (C) **1** and (D) **2**, MTT assay was done and percentage of cell viability was plotted. Data were transformed, normalized and IC_{50} values were calculated using Graph pad Prism. Data represents mean±SD of three independent experiments.

Such variations in cytotoxicity appear to be dependent on structural changes revealing some interesting trends that may help in understanding of the structure-activity relationship for further optimization of pharmacological index of pyrazole napthyl derivatives. Bridged dinuclear copper(II) complexes (**1** and **2**) having symmetric structure may provide a favourable electron transfer pathway to produce reactive oxygen species (ROS) from molecular oxygen that causes higher cytotoxicity effect. The monomeric [Co(A)Cl_2] (**3**) would be expected to be more lipophilic nature than the dinuclear **1** and **2** with better penetration of the cell wall. But the generation of ROS occurs at a lower rate which results a reduced cytotoxicity effect of **3** compared with copper(II) complexes.

An LDH assay was employed to differentiate apoptotic (programmed cell death) activity of these compounds from necrotic (cytolytic) activity. A higher dose of 50 µM was selected in this study to consider only the major cytolytic effect. Ligand A and **3** are causing more cytolysis than the two copper(II) compounds (Fig.10).

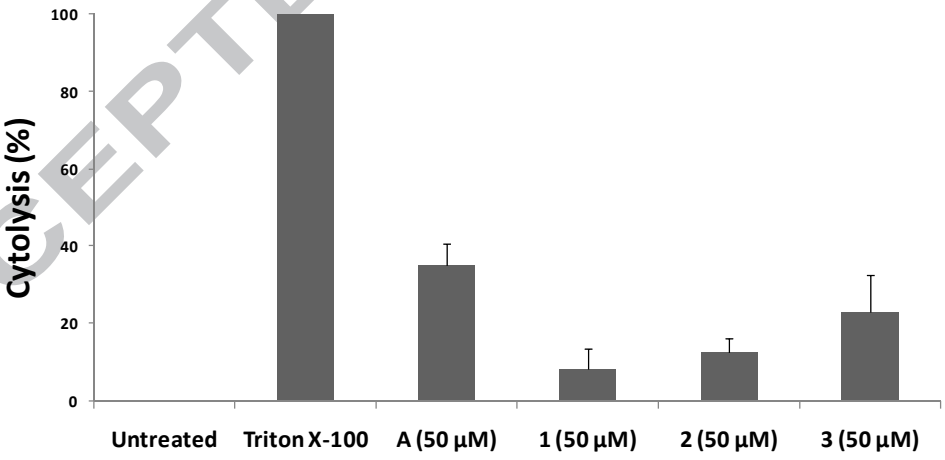

Fig. 10 Effect of compounds on cytolysis of U937 cells. U937 cells were treated for 24 h, with 50 µM of different copper compounds, culture supernatants were collected and assayed for lactate dehydrogenase (LDH). LDH release was plotted as percentage against triton X-100, which is considered as 100% and untreated cells were considered as 0%. Data represents mean ±SD of three independent experiments.

Cytolyses of the compounds are far less than triton X-100, which is known to lyse the cells completely. This data suggests that the mechanism of action of these two compounds might include both apoptosis and necrosis. Interestingly, **1** is most potent complex with an IC_{50} value of 13 ± 1 μM showing least cytolysis. This suggests that complex **1** predominantly follows the programmed cell death mechanism which is meaningful to be an active apoptotic inducer.

3.7 **DNA cleavage activity study**

Metal complexes are known to intercalate double-stranded DNA causing the breaks of the existing DNA structure which is known as chemical cleavage [20-22]. The chemical cleavage activity study was performed with freshly purified supercoiled plasmid DNA. If single strand breaks occur, the plasmid will change conformation to the nicked circular form which migrates at a slower rate than former. An increase in the nicked circular population is an indication for cleavage activity. Copper(II) complexes are known to intercalate into double- stranded DNA and cause DNA strands breakage [20-22]. Reducing and oxidizing conditions were kept to maintain different oxidation states of copper. Ligand A and **3** did not show much chemical cleavage activity both in the oxidizing and reducing environment. Excellent DNA chemical cleavage activity was shown by the dinuclear doubly bridged copper(II) complexes **1** (75%) and **2** (72%) only in the presence of the reducing agent GSH (Fig. 11A).

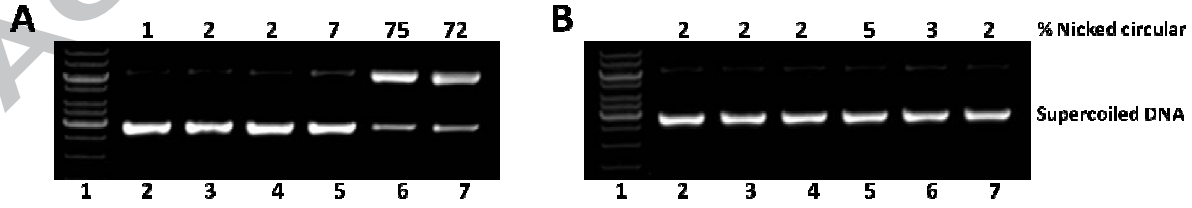

Fig. 11 DNA cleavage activity of compounds. Different copper compounds (10 μM) were incubated with 400 ng of pEGFP-C3 DNA for 2 h at 37^0C either in reducing environment consisting of 1 mM of reduced glutathione (A) or oxidizing environment consisting of 200 μM

of H_2O_2. Plasmids were run on 0.8% agarose gel. Figure A: lane 1–1 kb DNA marker, lane 2–DNA control, lane 3–DNA+GSH, lane 4–DNA+GSH+Ligand-A, lane 5– DNA+GSH+Complex-3, lane 6 – DNA+GSH+**1** and lane 7– DNA+GSH+2. Figure B is as same as Figure A, except that GSH was replaced by H_2O_2. Percentage of nicked circular was calculated using Image Quant software and indicated above.

The results show that bridged dinuclear compounds are more effective DNA cleavers than a generic monomeric cobalt(II) complex. This may be explained in terms of an inner sphere electron transfer (ISET) mechanism in the dinuclear species where the Cu(II) centers are reduced to Cu(I) through $\sigma^*(e_g)$ to $\sigma^*(e_g)$ electron transfer *via* a bridging Cl^- or azide ion in presence of glutathione [48]. The dinuclear bridged complex may acts as a preformed intermediate precursor in the said electron transfer mechanism following an electron injection from glutathione [48]. The dimeric bridged complexes are very effective generators of ROS through the rapid generation of Cu(I) species. The reduced copper(I) state readily takes up the oxygen molecule towards ROS generation. The conditions favouring the formation of Cu(I)-DNA are prerequisite to activation of oxidation damage to DNA by GSH and copper ion. The mechanism for monomeric cobalt(II) complex might not follow such reaction pathway which can cause DNA cleavage activity. The Co(II) center is chemically stubborn to reduce to Co(I). This is quite expected as the $E^0_{Co3+/Co2+}$ value (1.68 V) is higher than the $E^0_{Cu2+/Cu+}$ (0.38 V). The different steps of the ROS generation with intercalated copper complexes with DNA are given in the Scheme 4. The mechanism of the chemical nuclease activity is studied using different additives. The hydroxyl radical scavenger (DMSO and glycerol) and singlet oxygen quencher (sodium azide and histidine) were applied along with complex/ligand during DNA cleavage experiment (Fig.12).

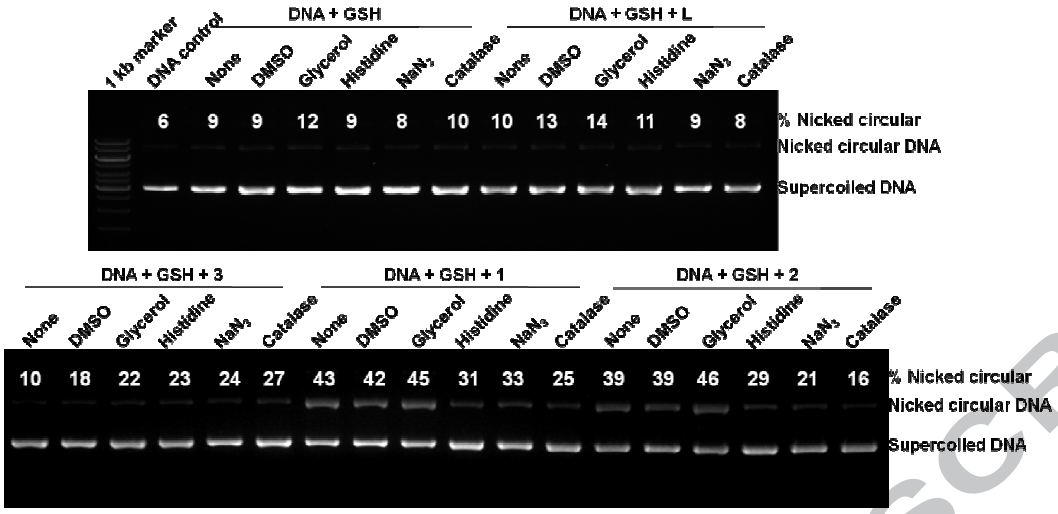

Fig. 12 Mechanistic studies of DNA cleavage activity of copper compounds. Different copper compounds (10 µM) were incubated with 400 ng of pEGFP-C3 DNA for 2 h at 37^0C in reducing environment consisting of 1 mM of reduced glutathione either alone or in presence of different ROS inhibitors (DMSO – 0.4 M, Glycerol –0.4 M, Histidine – 0.1 M, NaN_3 –0.1 M and Catalase –10 µg/ml). Plasmids were run on 0.8% agarose gel. Percentage of nicked circular was calculated using Image Quant software and indicated above.

The singlet oxygen quenchers protect more the DNA strand scission than hydroxyl ion scavengers [49, 50]. The former protects the DNA by about 70–80% while the later protect DNA by about 55–58%. This fact suggests that prior formation of $^1O_2$ or singlet oxygen like species occurred which could significantly bind the protein of DNA at onset of DNA scission. The hydroxyl ion or peroxide species were also formed when the reaction proceeded further.

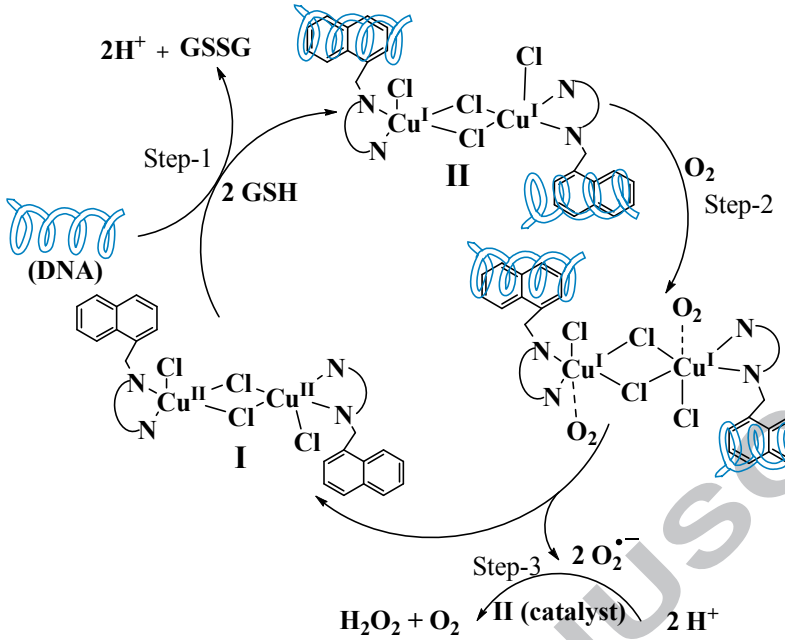

Scheme 4: Mechanistic cycle for reductive cleavage of DNA in presence of glutathione (GSH) in **1**.

$$2Cu(II) + 2DNA + 2GSH \xrightleftharpoons{\text{Step- 1}} 2Cu(I)\text{-}DNA + GSSG + 2H^+$$

$$2Cu(I)\text{-}DNA + 2O_2 \xrightleftharpoons{\text{Step- 2}} 2Cu(II) + DNA + 2\,O_2^{\bullet-}$$

$$2\,O_2^{\bullet-} + 2H^+ \xrightleftharpoons[2Cu(I)\text{-}DNA\ (catalyst)]{\text{Step- 3}} H_2O_2 + O_2$$

The planar napthyl group in the dinuclear complexes is responsible to bind the DNA through stacking mechanism [25, 51]. The groove binding property of the complexes through napthyl stacking facilitate the ISET mechanism to cleave the DNA. It is well documented that the redox active Cu(II) centre interacts with thiols (GSH) to form free thiyl radicals which subsequently dimerize to GSSG [52]. Cu(I)-DNA formation proceeds most easily when GSH interacts with Cu(II) in the vicinity of the DNA. Cu(I)-DNA is unstable in aerobic condition causing reductive

activation of O_2. This activation process actually forms H_2O_2 in presence of copper catalyst which is responsible for the generation of ROS and ultimately DNA damage occurs. The proposed DNA cleavage steps are given following Scheme 4 for the representative complex **1.** The contrasting result of the napthyl-pyrazole cobalt(II) complex (3) invariably note that the chemical nuclease activity mainly depends upon the presence of metal centres which are readily susceptible to reduction. The dinuclear copper(II) complexes show high chemical nuclease activity due to the presence of easily reducible bridged copper(II) centers. The presence of napthyl group does not induce any chemical nuclease activity in the mononuclear complex **3**. This complex is also devoid of a metal centre which can be reduced easily. Thus, we can conclude that the complexes having more than one metal centre show more significant DNA cleavage activity than a generic mononuclear complex.

3. Conclusion

Two new dinuclear bridged copper(II) complexes of (5-methyl- pyrazol-1-ylmethyl)-napthalen-1-ylmethyl-amine were successfully synthesized and characterized by means of available tools. The dissociation of parent ligand (A) and formation of stable bridged polynuclear copper(II) complexes with the derived ligand (L) enables strong intermolecular interactions in molecules. The complexes are more cytotoxic agents than the free ligand (A). The results demonstrate that the dinuclear copper(II) complexes (**1–2**) have higher cytotoxicity effect on U937 human monocytic cells than mononuclear cobalt(II) complex (**3**) and the free ligand A. Furthermore mononuclear $Co(A)Cl_2$ and ligand A did not show appreciable cleavage of plasmid DNA whereas the dinuclear bridged Cu(II) complexes **1** and **2** cleaved supercoiled plasmid DNA with 75 and 72%, respectively in the presence of reducing agent. The cobalt(II) center of **3** is not easily reducible in nature, so the generation of ROS is restricted. On the other hand, in the

dinuclear **1** and **2,** the Cu(II) centers are connected by μ-Cl and μ-N_3 bridges where fast electron transfer is possible through σ*(e_g) to σ*(e_g) orbital. The electron transfer may facilitate the formation of ROS in a reducing environment. The new symmetric dinuclear bridged copper(II) complexes with napthyl group have led to new potential copper drugs which can bind the DNA in reducing environment and behave as a good metallo-nuclease.

Acknowledgement:

We gratefully acknowledge the project grant no. 1 (2858)/16/EMR-II) from Council for Scientific and Industrial Research (CSIR), Government of India. Panskura Banamali College acknowledges the grants received from Department of Science and Technology (DST), Govt. of India through FIST program (SR-FIST-Col/295 dated 18/11/2015). We are also thankful to Dr. Debabrata Maity, Department of Chemistry, Indian Institute of Technology, Bombay, India and Dr. Santanu Pattanayak of National Chemical Laboratory, Pune, India for EPR spectroscopy. Panskura Banamali College acknowledge the grant from DST, Govt. of India (No.SR-FIST-COLLEGE-295-dt18/11/2015).

Appendix A. Supplementary data

CCDC 1551718 and 1551717 for compound **1** and **2,** respectively. Crystallographic data can be obtained free of charge on application to CCDC, 12 Union Road, Cambridge CB2 1EZ, UK fax (+44) 1223 336033, e-mail: deposit@ccdc.cam.ac.uk.

Conflict of interest

The authors declare no conflict of interest.

References

[1] J.Parez, L. Liera, Eur. J. Inorg. Chem. 33 (2009) 4913.

[2] R. N. Mukherjee, Coord. Chem. Rev. 203 (2000) 151.

[3] M. Sobiesiak, T. Muzioł, M. Rozalski, U. Krajewska, E. Budziszd, New J. Chem., 38 (2014) 5349.

[4] S. Bhattacharyya, A. Sarkar, S. K.Dey, G. P. Jose, A. Mukherjee, T. K. Sengupta, Dalton Trans. 42 (2013) 11709.

[5] S. Tardito, I. Bassanetti, C. Bignardi, L. Elviri, M. Tegoni, C. Mucchino, O. Bussolati, R. Franchi-Gazzola, L. Marchiò, J. Am. Chem. Soc. 133 (2011) 6235.

[6] K. M. Szécsényi, V. M. Leovac, V. I. Cesljevic, A. Kovacs, G. Pokol, G. Argay, A Kálmán, G. A. Bogdanović, Ž. K. Jaćimović, A. S. Biré, Inorg. Chim .Acta. 353 (2003) 253.

[7] C. D. Fan, H. Su, J. Zhao, B. X. Zhao, S. L. Zhang, J. Y. Miao, Eur. J. Inorg. Chem. 45 (2010) 1438.

[8] A. Santra, G. Mondal, M. Acharjya, P. Bera, A. Panja, T. K. Mandal, P. Mitra, P. Bera, Polyhedron 113 (2016) 5.

[9] M. C. Linder, Biochemistry of Copper, Plenum Press, New York., 1991.

[10] S. Tardito, I. Bassanetti, C. Bignardi, L. Elviri, M. Tegoni, C. Mucchino, O. Bussolati, R. Franchi-Gazzola, L. Marchio, J. Am. Chem. Soc. 33 (2011) 6235.

[11] R. Krikavora, J. Vanco, Z. Travinicek, R. Buchtik and Z. Dvorak, RSC Adv.,6 (2016) 3899.

[12] W. Zhou, X. Wang, M. Hu, C. Zhu, Z. Guo, Chem. Sci. 5 (2014) 2761.

[13] S. Tardito, A. Barilli, I. Bassanetti, M. Tegoni, O. Bussolati, R. Franchi-Gazzola, C. Mucchino, L. Marchio, J. Med. Chem. 55 (2012) 10448.

[14] D. Palanimuthu, S. V. Shinde, K. Somasundaram, A. G. Samuelson, J. Med. Chem. 56 (2013) 722.

[15] C. Marzano, M. Pellei, F. Tisato, C. Santini, Anti-Cancer Agents Med. Chem., 9 (2009) 185.

[16] C. Santini, M. Pellei, V. Gandin, M. Porchia, F. Tisato, C. Marzano, Chem. Rev. 114 (2014) 815.

[17] E. C. M. O. Weiker, M. A Siegler, M. Lutz, E. Bouwman, Dalton Trans. 44 (2015) 12196.

[18] M. Grazul, E. Besic-Gyenge, C. Maake, M. Ciolkowski, M. Czyz, R. K.O. Sigel and E. Budzisz, J. Inorg. Bio. Chem. 135 (2014) 68.

[19] L. Q. Hatcher, K. D. Karlin, J. Biol. Inorg. Chem. 9 (2004) 669.

[20] K. J. Humphreys, K. D. Karlin, S. E. Rokita, J. Am. Chem.Soc. 124 (2002) 6009.

[21] K. J. Humphreys, K. D. Karlin, S. E. Rokita, J. Am. Chem. Soc. 124 (2002) 8055.

[22] K. J. Humphreys, K. D. Karlin and S. E. Rokita , J. Am. Chem. Soc. 123 (2001) 5588.

[23] L. Li, N. N. Masthy, J. Tesser, L. N. Zakharov, G. P. A. Yap, A. L. Rhensold, K. D. Karlin, S. E. Rokita, Inorg. Chem. 45 (2006) 7144.

[24] Y. Jin, J. A. Cowan, J. Am. Chem. Soc. 127 (2005) 8408.

[25] B. Macias, M. V. Villa, B. Gomez, J. Borras, G. Alzuet, M. González-Álvarez, A. Castineiras, J. Inorg. Bio. Chem. 101 (2007) 444.

[26] W. R. Browne, R. Hage, J. G. Voc, Coord. Chem. Rev. 250 (2006) 1653.

[27] W. Kaimand and B. Sarkar, Coord. Chem. Rev. 251 (2007) 584.

[28] A. Panja, P. Guionneau, *Dalton Trans*. 49 (2013) 5068.

[29] S. Gama, F. Mendes, F. Marques, I. C. Santos, M. F. Carvalho, I. Correia, J. C. Pessoa, I. Santos, A. Paulo, J. Inorg. Bio. Chem. 105 (2011) 637.

[30] M. R. Malachowski, M. G. Davidson, Inorg. Chim. Acta. 162 (1989) 199.

[31] I. Banerjee, J. Marek, R. Herchel, M. Ali, Polyhedron 29 (2010) 1201.

[32] A. Jana, M. Dolai, B. K. Shaw, S. K. Saha, M. Ali, Transition. Met. Chem. 3 (2016) 347.

[33] G. M. Sheldrick, G. M, CELL NOW, program for unit cell determination, University of Göttingen, Germany, 2005 & Bruker AXS Inc, Madison (WI), USA, 2005.

[34] A. Altomare, M. C. Burla, M. Camalli, G. L. Cascarano, C. Giacovazzo, A. Guagliardi, A. G. G. Moliterni, G. Polidori, R. Spagna, J. Appl. Crystallogr. 32 (1999) 115.

[35] L. Krause, R. Herbst-Irmer, G. M. Sheldrick, D. Stalke, J. Appl. Cryst. 48 (2015) 3.

[36] G. M. Sheldrick, Twinabs, Bruker AXS scaling for twinned crystals, version 2007/3, and Sadabs, Bruker AXS area detector scaling and absorption correction, version 2007/2, University of Göttingen, Germany, 2007 and Bruker AXS Inc, Madison (WI), USA, 2007.

[37] G. M. Sheldrick, SHELX2013 – Programs for Crystal Structure Analysis (Release 97-2), Institöt für Anorganische Chemie der Universität, Tammanstrasse 4, D-3400 Gttingen, Germany., 2013.

[38] J.A.P. M. J. Frisch, G. W. Trucks, H. B. Schlegel, G. E. Scuseria, M. A. Robb, J. R. Cheeseman, J. A. Montgomery, T. Vreven, K. N. Kudin, J. C. Burant, J. M. Millam, S. S. Iyengar, J. Tomasi, V. Barone, B. Mennucci, M. Cossi, G. Scalmani, N. Rega, G. A. Petersso, Gaussian 03 Package., 2003.

[39] R. B. Mokhamatam, B. K. Sahoo, S. K. Manna, Apoptosis 21 (2016) 928.

[40] S. Bhattacharyya, T. J. R. Weakley, M. Chaudhury, Inorg. Chem. 38 (1999) 5453.

[41] S. Bhattacharyya, T. J. R. Weakley, M. Chaudhury, Inorg. Chem. 38 (1999) 633.

[42] M. R. Malachowski, A. S. Kasto, M. E. Adams, A. L. Rheingold, L. N. Zakharov, L. D. Margerum, M. Greaney, Polyhedron 28 (2009) 393.

[43] H. Yang, Y. Tang, Polyhedron 28 (2009) 3491.

[44] B. Sarkar, S. Konar, C.J. Gomez-Garcia, A. Ghosh, Inorg. Chem. 47 (2008) 11611.

[45] A. Domenech, E. G. Espana, P. Navarroc, C. Mirandac, Dalton Trans., 2006, 4926–4935.

[46] J. L. Garcia-Gimenez, G. Alzuet, M. Gonzalez-Alvarez, A. Castineiras, M. Liu-Gonzalez, J. Borras, Inorg. Chem. 46 (2007) 7178.

[47] A. W. Addison, T. N. R. J. Reedijk, J. V. Rijn, G. C. Verschoor, J. Chem. Soc., Dalton Trans. (1984) 1349.

[48] Mechanisms of Inorganic Reactions. A Study of Metal Complexes in Solution. Fred Basolo, Ralph G. Pearson. Wiley, New York, Ed. 2, 1967.

[49] P. Naveen, R. Jain, P. Kalaivani, R. Shankar, F. Dallemer, R. Prabhakaran, New J. Chem. 41 (2017) 8885.

[50] T. K. Goswami, B. V. Chakravarthi, M. Roy, A. A. Karande, A. R. Chakravarty, Inorg. Chem. 50 (2011) 8452.

[51] X. Q. Zhou, Q. Sun, L. Jiang, S. T. Li, W. Gu, J. L. Tian, X. Liu, and S. P.Yan, Dalton Trans. 44 (2015) 9516.

[52] W. A. Prutz, Biochem. J. 302 (1994) 373.

Synthesis, Characterization, Cytotoxicity Effect and DNA Cleavage Study of Symmetric Dinuclear Chloro and Azido Bridged Copper(II) Complexes of Napthyl-pyrazole Based Ligand

Abhimanyu Jana, Paula Brandão, Gopinath Mondal, Pradip Bera, Ananyakumari Santra, Atish Dipankar Jana, Raveendra Babu Mokhamatam, Sunil Kumar Manna, Nandan Bhattacharyya, Pulakesh Bera*

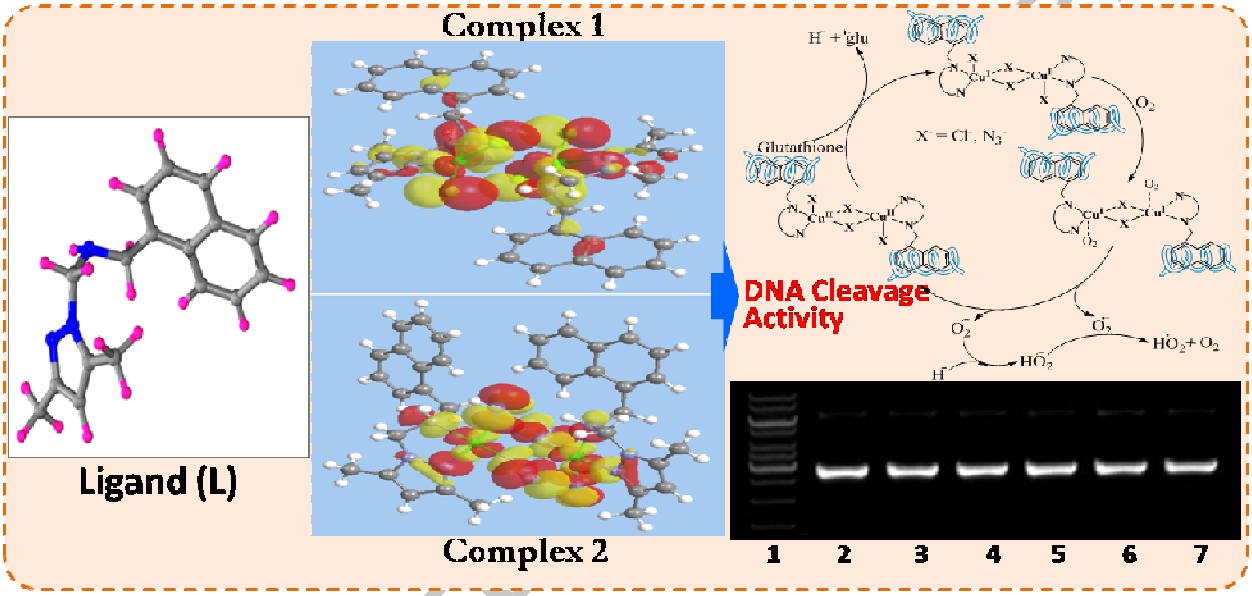

Highlights

(a) Synthesis of new napthyl-pyrazole ligand with biological potentiality

(b) Preparation of symmetric dinuclear chloro and azido bridged Cu(II) complexes

(c) Complexes are structurally characterized and additionally DFT, CV and EPR studies were done

(d) Cytotoxicity effect, DNA cleavage activities of the new compounds

(e) Rational discussion on structure-activity relationship will be accounted by the scientific community.